A New Family of Insulin-Mimetic Vanadium Complexes Derived from 5-Carboalkoxypicolinates

Jessica Gätjens,[a] Beate Meier,[b] Tamás Kiss,[c] Eszter M. Nagy,[c] Peter Buglyó,[d] Hiromu Sakurai,[e] Kenji Kawabe,[e] and Dieter Rehder*[a]

Abstract: The reaction of 5-carboalkoxypicolinic acid (5ROpicH, R = Me, Et, *i*Pr, *s*Bu; **1a–d**) with vanadyl sulfate yielded the complexes $[VO(H_2O)(5R\text{-}Opic)_2]$, **2a–d**, with H_2O and one of the picolinato ligands in the equatorial positions, and the second picolinate occupying equatorial (*N*) and axial (*O*) positions. Reaction of **1a** with $[NH_4][VO_3]$ yielded $[NH_4][VO_2(5\text{-}MeOpic)_2]$, $[NH_4]$-**3**, in which the *N* functions of the picolinates are *trans* to the doubly bonded, *cis*-positioned oxo groups. Complexes **1a**·H_2O, **1b**, **1c**, **2a**·$3.5\,H_2O$ and $[NH_4]$-**3**·$4\,H_2O$ have been structurally characterised. A detailed pH-potentiometric solution speciation analysis of the system VO^{2+}-**1a** revealed a dominance of $VO(5OMepic)_2$ between pH 2 and 6, with the same coordination pattern, evidenced by EPR spectroscopy, as in the crystalline solid state. In ternary systems containing physiological concentrations of the low molecular mass biogenic binders (B) lactate, oxalate, citrate or phosphate, ternary species of general composition VO(5MeOpic)B dominate at physiological pH, with citrate being the most effective competitor for picolinate. All of the complexes trigger glucose uptake and degradation by simian virus modified mice fibroblasts at non-toxic concentrations ($<100\,\mu$M), with **2a**, $[VO_2(pic)_2]^-$ and $[VO_2(dipic)]^-$ being at least as effective as insulin. Vanadium uptake by the cells is most effective in the case of **2a**. **2a** also effectively inhibits free fatty acid release by rat adipocytes treated with epinephrine, thus mimicking the inhibition of lipolysis by insulin.

Keywords: bioinorganic chemistry · diabetes · picolinates · solution speciation · vanadium

Introduction

The use of sodium metavanadate in the treatment of human diabetes mellitus had already been reported as early as 1899,[1] but interest in pharmaceutically available insulin substitutes containing vanadium has revived only during the last 25 years.[2–4] Efforts have been made to design coordination compounds of vanadium in the oxidation states +IV and +V[5] (and, more recently, also +III[6]) that exhibit insulin-mimetic activities and, concomitantly, low toxicity. Vanadate itself is toxic due to its inhibitory effect towards various phosphate-metabolising enzymes.[7] The main advantage of vanadium compounds, as compared to insulin, lies in the possibility of oral administration. Furthermore, vanadium compounds are active in type 1 diabetes (which is due to insufficient or lacking insulin supply) *and* type 2 diabetes (non-insulin-dependent diabetes mellitus, due to insulin resistance).

The insulin-like activities exhibited by vanadium compounds encompass the ability to lower elevated blood glucose levels in vivo. Vanadium stimulates glucose uptake and subsequent oxidation in glucose-metabolising cells as well as glycogen synthesis in vitro. In addition, it promotes the inhibition of glycolysis and glyconeogenesis, and inhibits lipolysis (activates lipogenesis).

To be therapeutically effective, a compound should exhibit a balanced lipophilicity and hydrophilicity, which can be achieved by an appropriate design of the periphery of the coordination compound, thereby providing facile uptake by and transport in the bloodstream. The complexes should further be stable with respect to ligand exchange in order to survive the acidic conditions in the stomach and the transport

[a] Prof. Dr. D. Rehder, Dipl.-Chem. J. Gätjens
Institute of Inorganic and Applied Chemistry
University of Hamburg, 20146 Hamburg (Germany)
[b] Prof. B. Meier
BCM-Research Institute
85307 Entrischenbrunn (Germany)
[c] Prof. T. Kiss, E. M. Nagy
Department of Inorganic and Analytical Chemistry
University of Szeged, 6701 Szeged (Hungary)
[d] Dr. P. Buglyó
Department of Inorganic and Analytical Chemistry
University of Debrecen, 4010 Debrecen (Hungary)
[e] Prof. Dr. H. Sakurai, K. Kawabe
Department of Analytical and Bioinorganic Chemistry
Kyoto Pharmaceutical University, Kyoto, 607-8414 (Japan)

DOI: 10.1002/chem.200305019

by body fluids. To facilitate efficient transport across hydrophobic membranes into the target cell, the ligand sphere should also contain a site for recognition by a membrane receptor. Finally, non-toxic metabolites are advantageous. This latter requirement is fulfilled with picolinic acid (pyridine-2-carboxylic acid), which is an intermediate in the tryptophane degradation path way.

Promising results with regard to the aspects mentioned above have thus been obtained with vanadium complexes bearing ligands derived from picolinic acid, picH. These ligands form vanadium compounds with the *NO*, *OO* or *ONO* coordination modes; for an early review by J. Selbin reference [8]. Complexes with vanadium in oxidation state +IV and picolinate as ligand, $[VO(pic)_2]$, were initially tested for their insulin-like activity in 1995 by Sakurai and co-workers, who demonstrated the ability of these complexes to normalise both serum glucose and free fatty acid (FFA) levels in rats.[9] Starting from these results, various V^{IV} and V^{V} compounds with picH and derivatives of picH were the subject of research activities in terms of their insulin-mimetic (normoglycemic) activity. Examples are complexes with picolineamides,[10] and picolinates with the substituents 5-I,[11] 6-Me, 6-COO^- (dipic),[10, 12, 13] 6-Et[14, 15] and 4-OH-dipic.[16, 17] It is noteworthy that the oxidation state of vanadium does not seem to play a crucial role in activity.[18] The complex anion $[VO_2(dipic)(H_2O)]^-$ proved promising in the oral treatment of diabetic cats.[19, 20] The peroxo complex $K_2[VO(O_2)_2pic]$ has been shown to decrease blood glucose levels in streptozotocin-induced diabetic rats.[21] Apart from the various picolinato vanadium compounds, there also exist several examples for picolinato complexes with metal centres other than vanadium, such as zinc, cobalt and chromium, which have also been shown to be insulin-mimetic.[3, 21]

Here, we present a novel variant of the picolinato scheme, with regard to vanadium complexes of 5-carboalkoxypicolinic acid, 5ROpicH (Scheme 1), with a site for modification, with respect to the substituent R in the 5-position, which allows a fine tuning of the properties of the respective vanadium complexes in the periphery of the coordination sphere.

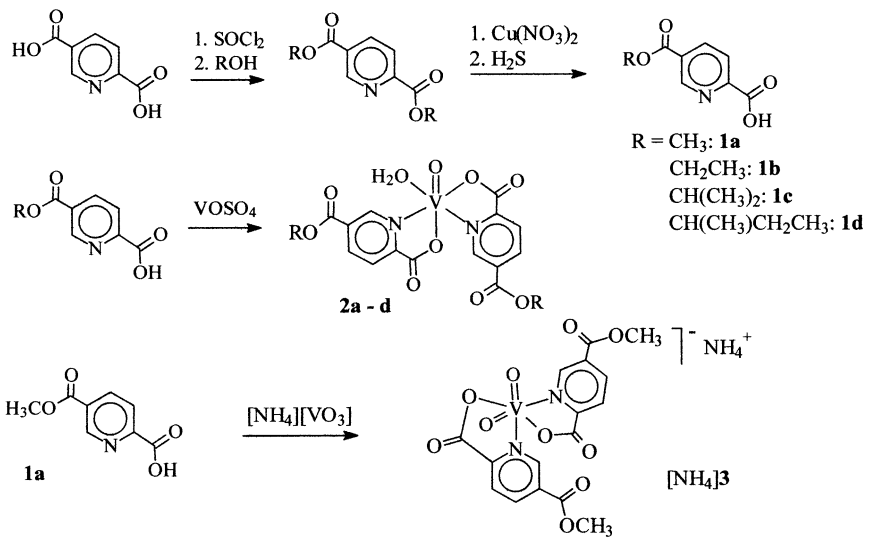

Scheme 1.

Results and Discussion

Synthesis, characterisation and structure description: Scheme 1 provides an overview of the ligands and complexes introduced here. For the syntheses of the 5-carboalkoxypicolinic acids, 5ROpicH (**1a**–**d**), the pyridine-2,5-dicarboxylic acids were converted to the dialkylesters according to known procedures.[14] Reaction with copper(II) nitrate yielded blue copper complexes, from which the monoesters were liberated with hydrogen sulphide.[15] In the case of **1a**, **1b** and **1c** single crystals were grown out of aqueous acetone. The acids crystallise in the triclinic space group $P\bar{1}$ (**1a**·H_2O, **1b**) or in the monoclinic space group $P2(1)/c$ (**1c**). The molecular structures and sections of the crystal structures showing the H-bonding network are depicted in Figure 1. Bond lengths and angles (Table 1) are in the expected range. In **1a**·H_2O, adjacent molecules of **1a** are linked together through two water molecules by hydrogen bridges; the water molecules act as donors to the pyridine-*N* and as acceptors for the carboxylic-OH, giving rise to chains consisting of H_2O-bridged dimers of **1a**. These chains are interlinked by hydrogen bonds between water and the carboxylic-*O*. In **1b**, trimeric subunits are formed by OH···*N* links, while in **1c**, the molecules are infinitely linked through OH···*N* hydrogen bonds.

For the syntheses of the vanadium(IV) complexes **2a**–**d**, an aqueous solution of vanadyl sulfate was mixed with a solution of 5ROpicH and sodium acetate in water/THF and heated to 50 °C for 2 h. The complexes precipitated in the form of green, microcrystalline powders. Once generated, the complexes are stable in air. Elemental analyses confirmed the expected coordination of two molecules of the ligand to the metal centre, with the sixth position occupied by a molecule of water. In the case of $[VO(H_2O)(5MeOpic)_2]$ (**2a**), green single crystals of **2a**·3.5H_2O were obtained from a hot aqueous solution by slow cooling. The yellow bis(oxo)vanadium(V) complex $[NH_4][VO_2(5MeOpic)_2]$, [NH_4]-**3**, was obtained by mixing a slurry of $[NH_4][VO_3]$ in water with a solution of the 5MeOpicH in acetone. Single crystals of [NH_4]-**3**·4H_2O suitable for an X-ray diffraction analysis were grown from the mother liquid. The molecular structure of $[VO(H_2O)(5MeOpic)_2]$ (**2a**) is displayed in Figure 2, with bonding parameters in Table 2 and, for the ligand, in Table 1. The asymmetric unit contains two independent molecules and seven waters of crystallisation. The basic formula of the crystalline material thus is **2a**·3.5H_2O and crystallises in the triclinic space group $P\bar{1}$, while the bulk material, as evidenced by the elemental analysis and thermogravimetry (vide infra), is free of water of crystallisation. In one of the independent

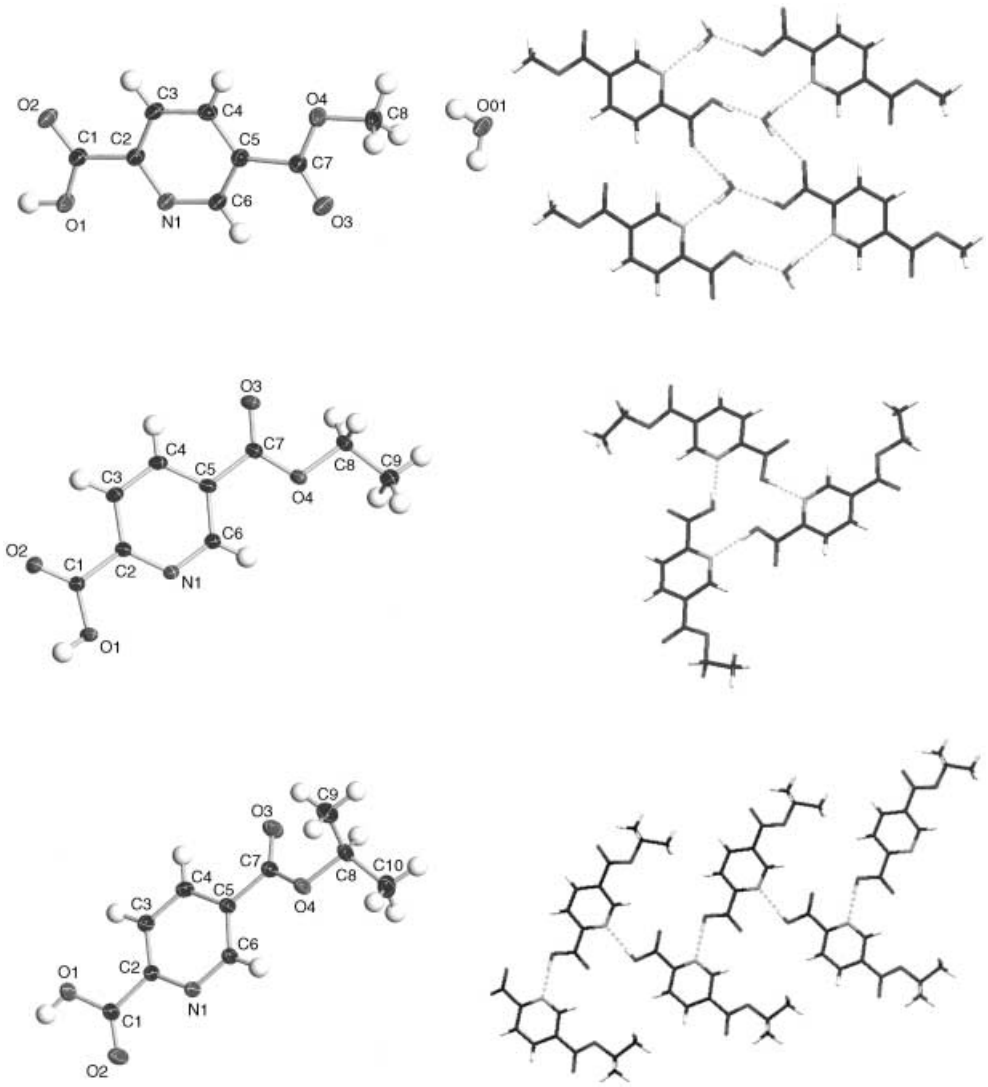

Figure 1. XSHELL plots (50% probability level) of **1a**·H_2O, **1b** and **1c**.

molecules, the methoxy group is disordered over two positions (70:30%). Four of the waters of crystallisation are disordered as well. See also Experimental Section for disorder information. The ligands coordinate in the usual bidentate manner, forming, together with an aqua ligand (O2) in the equatorial and the doubly bonded oxygen (O1) in the apical position, a complex of distorted octahedral geometry. The second axial position is occupied by the carboxylate oxygen O7 of one of the picolinates. The corresponding bond length *d*(V1−O7), 2.122(3) Å, is rather long as a consequence of the *trans* influence of O1. The angle O1-V-O7, 165.1(1)°, significantly deviates from linearity, possibly as a result of the steric hindrance imparted by one of the carbomethoxy groups. Vanadium is displaced from the equatorial plane spanned by N1, N2, O2 and O3 towards the apical O1 by 0.295 Å. Water of crystallisation is hydrogen-bonded to the aqua ligand and the coordinated carboxylate-oxygen atoms O3 and O7, and further forms a weak bond to the methoxy group O5; Table 2. The ligand bonding parameters (Table 1) are the same within the limits of error as in the free acids, with the exception of the bond length carboxylate-OH (C1−O1 in **1a**, which is somewhat longer than for the deprotonated, coordinated carboxylate-*O* (C1−O3 and C9−O7) in **2a**.

$[NH_4][VO_2(5MeOpic)_2]\cdot 4H_2O$ ([NH_4]-**3**·$4H_2O$) (Figure 3 and Table 2) crystallises in the monoclinic space group *C*2/*c*. Two of the water molecules are disordered, one to the extent where it is displaced along the C_2 axis across the space between the facing VO_2 moieties of two neighbouring anions; Figure 3, right. The molecular structure is shown in Figure 3, left. The oxo groups (O5, O5A) are *cis* standing, bisected by the C_2 axis which passes through the vanadium centre and the octahedral edge formed by N1 and N1A. In contrast to **2a**, where a carboxylate-*O* is *trans* to the oxo group, the pyridine-*N* are *trans* to the oxo groups in **3**, giving rise to rather long *d*(V−N1) = 2.310(2) Å. The molecular axis, defined by O5-V-N1, is again tilted: the angle is 163.42(7)°. Vanadium is above

Table 1. Selected bond lengths [Å] and angles [°] for **1a**·H_2O, **1b** and **1c**, and the ligand **1a**(1 –) in the complexes **2a** and **3**.

	1a·H_2O	**1a**$^-$ in **2a**·3.5H_2O	**1a**$^-$ in [NH_4]**3**·4H_2O	**1b**	**1c**
C1–C2	1.5058(18)	1.511/1.502(5) C1–C2/C9–C10	1.504(3) C1–C2	1.5093(17)	1.5064(14)
C1–O1	1.3110(16)	1.304/1.279(5) C1–O3/C9–O7	1.284(2) C1–O1	1.3066(15)	1.3188(13)
C1–O2	1.2148(16)	1.232/1.232(4) C1–O4/C9–O8	1.226(2) C1–O2	1.2117(15)	1.2068(14)
C5–C7	1.4984(19)	1.498/1.481(5) C5–C7/C13–C15	1.490(3) C5–C7	1.4928(17)	1.4920(14)
C7–O3	1.2009(17)	1.208/1.209(4) C7–O5/C15–O9	1.195(3) C7–O3	1.2111(15)	1.2079(13)
C7–O4	1.3323(16)	1.327/1.324(5) C7–O6/C15–O10	1.318(3) C7–O4	1.3292(15)	1.3336(13)
C8–O4	1.4543(17)	1.456/1.454(5) C8–O6/C16–O10	1.464(3) C8–O4	1.4622(15)	1.4688(12)
O1-C1-O2	125.37(12)	126.6/124.9(4) O3-C1-O4/O7-C9-O8	124.29(19) O1-C1-O2	125.93(11)	125.84(10)
O3-C7-O4	124.56(12)	124.7/124.9(4) O5-C7-O6/O9-C15-O10	123.8(2) O3-C7-O4	124.45(11)	124.91(10)
C7-O4-C8	114.91(11)	115.3/115.7(3) C7-O6-C8/C15-O10-C16	116.2(18) C7-O4-C8	114.27(10)	116.19(8)
O1···O01	2.52				
O01···O2	2.77				
O01···N1	2.83				
O1···N1				2.70	2.72

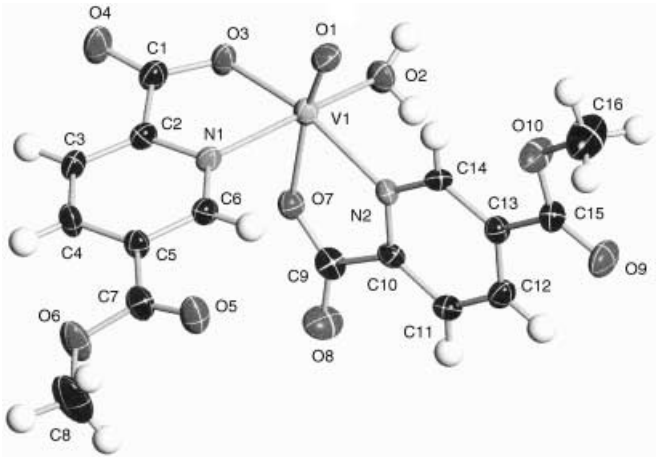

Figure 2. XSHELL plot (50% probability level) of **2a**. Only one of the two independent molecules is shown.

Table 2. Selected bond lengths [Å] and angles [°] for **2a**·3.5H_2O and [NH_4]-**3**·4H_2O.[a]

2a·3.5H_2O		[NH_4]-**3**·4H_2O	
V1–O1	1.597(3)	V1–O5	1.6287(14)
V1–O2	2.016(3)		
V1–O3	1.989(3)	V1–O1	1.9784(14)
V1–O7	2.122(3)		
V1–N1	2.118(3)	V1–N1	2.3098(16)
V1–N2	2.133(3)		
O1-V1-O7	165.04(12)	O5-V1-N1	163.42(7)
O2-V1-N1	161.37(13)	O1-V1-O1A	150.13(8)
O3-V1-N2	163.31(12)	O5-V1-O5A	105.68(11)
O3-V1-N1	78.71(11)	O1-V1-N1	73.83(5)
O7-V1-N2	74.53(11)		
O2···O21	2.600(5)	O10···O3	2.803(3)
O2···O22	2.688(5)	O10···O5	2.896(2)
O21···O7	2.832(5)	N2···O2	2.927(2)
O22···O3	2.886(5)	N2···O10	2.843(2)
O23···O5	3.065(6)		

[a] O21, O22 and O10 correspond to water of crystallisation.

the plane spanned by O1, O1A, N1A and O5A by 0.296 Å. The *d*(V–O5), 1.629(1) Å, are relatively long, possibly as a consequence of the hydrogen bonding to water of crystallisation, O10, and reflected in the rather low value ν(V=O); see Table 3. O10 is further hydrogen-bonded to the ammonium cation, which in turn forms a hydrogen bond to the non-coordinated carboxylate-O2. In addition, O3 of the ester group forms hydrogen bonds with interstitial water. The ligand parameters compare to those of the free picolinic acid, except again for a shortening of *d*(C1–O1) in **3** as compared to **1a**, Table 1.

Selected IR data are collated in Table 3. The C=O stretch is somewhat strengthened in the complexes, reflected by a shift to higher wavenumbers by approximately 15 cm^{-1} in the complexes with respect to the free ligands. The difference

Table 3. Selected IR[a] data.

	1a	**1b**	**1c**	**1d**	**2a**	**2b**	**2c**	**2d**	**3**
ν(C=O)	1719, 1698	1717, 1697 sh	1717	1714	1733	1737	1730	1729	1732
$\nu(CO_2)_{as}$					1654	1651	1652	1650	1658
$\nu(CO_2)_{sym}$					1397	1402	1397	1403	1396
ν(V=O)					971	978	967	967	903br

[a] KBr, in cm^{-1}.

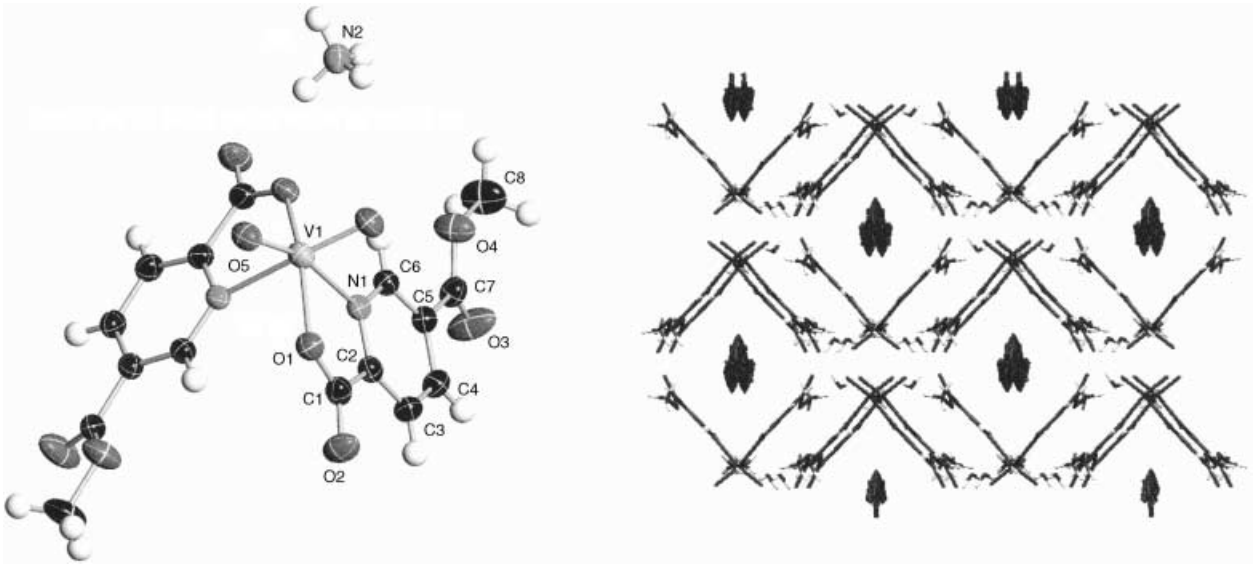

Figure 3. Molecular structure (left; 50% probability level) and section of the crystal structure (right) of $[NH_4]$-**3**$\cdot 4H_2O$.

between the antisymmetric and symmetric carboxylate bands corresponds to what one expects for the monodentate coordination of carboxylates. The V=O stretch is normal for the VO^{2+} complexes **2a**–**d**; it is rather low for the VO_2^+ complex **3**, which may be due to the above-mentioned intimate hydrogen bonding to water of crystallisation.

Thermogravimetry shows the loss of one H_2O molecule (4.1%) at 130 °C, which is typical for vanadyl complexes containing an equatorially coordinated aqua ligand.[25] The first ligand is degraded between 240 and 380 °C, the second around 500 °C. The overall weight loss due to ligand degradation amounts to 69.7%, that is, part of the picolinate ligands (corresponding to 4H, 2O, and 1N) remains on vanadium, which is recovered in the form of $[NH_4][VO_3]$. The third oxygen necessary to generate metavanadate apparently stems from external oxygen.

Solution speciation studies: To assess the stability of the complexes under various pH conditions and in the presence of competitive low molecular mass ligands present in the blood serum (oxalate, lactate, citrate, phosphate), we have carried out speciation studies for the systems containing 5-methylcarboxy-picolinic acid (**1a**; abbreviated AH in the context of the speciation studies) by pH potentiometry. Binding modes of the complexes in solution were determined by EPR spectroscopy.[26] The results are represented in Table 4, and in Table 5 in more detail for the binary VO^{2+}-AH system. According to these findings, the species $[VOA_2]$, which dominate over a wide pH range (vide infra), attain the same ligand distribution as is found for the solid state structure; see **2a** in Figure 2 and Scheme 1.

The protonation constants ($\log K$) for **1a**, and the stability constants for the complexes ($\log\beta$) are listed in Table 6, together with those of picolinate and 6-methylpicolinate[27, 28] for comparison (see Experimental Section for notation). The presence of the carbomethoxy group in **1a** significantly decreases the basicity of both protonation sites, the pyridine-*N* and the carboxylate, as a consequence of the electron-withdrawing effect of the ester group. Compound **1a**, similar to picH and 6MepicH, forms mono- and bis(ligand) complexes of different protonation states with VO^{2+} (Table 6 and Figure 4). The stability constants for the complexes formed with **1a**$(1-)$ are about the same as those for 6Mepic$(1-)$.

Table 4. EPR parameters and suggested binding sets for the complexes formed in the binary system VO^{2+}-5MeOpicH (AH) and the ternary systems VO^{2+}-AH-BH_n, BH_n = oxalic/lactic/citric/phosphoric acid.

Species[a]	g_z	A_z (10^{-4} cm^{-1})	Ligand sets[b]
$[VOA]^+$ I	1.939	179	(N, CO_2^-)
cis-$[VOA_2]$ II	1.947	168	(N, CO_2^-); (N, $CO_2^-{}_{ax}$); H_2O
$[VOAH_{-1}]^-$ III	1.947	171	(N, CO_2^-); H_2O; OH^-
$[VOAH_{-2}]^{2-}$ IV	1.948	167	(N, CO_2^-); OH^-; OH^-
oxalic acid			
cis-$[VOAB]^-$	1.943	170	(N, CO_2^-); (CO_2^-, $CO_2^-{}_{ax}$); H_2O
lactic acid			
cis-[VOAB]	1.946	166	(N, CO_2^-); (CO_2^-, OH_{ax}); H_2O
citric acid			
$[VOAB]^{2-}$	1.945	169	(N, CO_2^-); (CO_2^-, OH, $CO_2^-{}_{ax}$)
$[VOABH_{-1}]^{3-}$	1.948	159	(N, CO_2^-); (CO_2^-, O^-, $CO_2^-{}_{ax}$)
phosphoric acid			
$[VOABH_x]^{(2-x)-}$, x = 2,1,0	1.940	177	(N, CO_2^-); $H_xPO_4^{(3-x)-}$; H_2O

[a] See also Table 5 for the species I–IV; *cis* refers to the position of the aqua ligand (*cis* with respect to the doubly bonded O). [b] Equatorial, if not indicated otherwise.

Table 5. EPR parameters of the binary system VO^{2+}-5MeOpicH (AH).

pH	Species[a] (ratio[b])	*g* value			*A* value (10^{-4} cm^{-1})		
		g_0	g_z	g_{xy}	A_0	A_z	A_{xy}
1.85	I (90%)	1.968	1.939	1.982	96.7	179.8	55.1
	II (10%)	1.968	1.947	1.978	96.7	168.0	61.0
4.05	I (60%)	1.970	1.939	1.986	91.9	179.1	48.2
	II (40%)	1.970	1.946	1.983	91.9	168.4	53.6
6.00	III (100%)	1.972	1.947	1.985	93.9	171.0	55.4
7.42	IV (100%)	1.971	1.948	1.983	90.4	167.6	51.8
8.80	IV (100%)	1.972	1.948	1.985	89.5	166.7	50.9

[a] See Table 4. [b] Roughly estimated from peak height.

Table 6. Protonation constants ($\log K$), and stability constants for the complexes ($\log\beta$) formed between VO^{2+} and A(H) at 25 °C and $I = 0.2$ M (3σ errors in parentheses).

	5MeOpicH, **1a**	picH[b]	6MepicH[b]
$\log K$(HA)[a]	3.35(1)	5.19	5.82
$\log\beta[VOA]^+$	5.16(4)	6.66	5.13
$\log\beta[VOH_{-1}A]$	0.38(4)	–	–
$\log\beta[(VO)_2H_{-2}A_2]$	3.75(4)	6.15	3.25
$\log\beta[VOH_{-2}A]^-$	−6.8(2)	–	−6.56
$\log\beta[VOA_2]$	9.52(4)	12.11	9.28
$\log K(VOA_2)$	4.36	5.45	4.15
$\log K(VOA/VOA_2)$	0.80	1.21	0.98
$\log K$ for $VO^{2+} + HA = [VOA]^+ + H^+$	1.81	1.47	−0.69
$\log K$ for $VO^{2+} + 2HA = [VOA_2] + 2H^+$	2.82	1.73	–2.36

[a] Protonation site for the pyridine-*N*. The $\log K$ for the protonation of the carboxylate is ≈ 1 for picH and 6MepicH, and < 1 for 5MeOpicH. [b] From ref. [27].

However, the equilibrium constants for the proton displacement reactions shown in the two last rows in Table 6 clearly indicate that **1a**(1 −) coordinates to VO^{2+} significantly more readily than 6Mepic(1 −). This should be mainly due to the steric hindrance of the methyl group adjacent to the pyridine-*N* in the latter.[27, 28] Figure 4 shows that the mono- and bis(ligand) species form simultaneously, with $[VOA_2]$ dominating the pH range 2–6. In the pH range 5–7, deprotonation (of aqua ligands) is accompanied by an about 50% intensity loss of the EPR signal. This can be interpreted by the formation of the EPR silent, hydroxo-bridged dinuclear $[(VO)_2H_{-2}A_2]^{2-}$ species along with the mononuclear $[VOH_{-1}A]^-$. On further increasing the pH, deprotonation proceeds by formation of $[VOH_{-2}A]^{2-}$ (species IV in Table 4), until finally ligand-free and EPR-silent vanadylhydroxides of higher nuclearity are generated.

Due to their high affinity for hard (oxophilic) metal ions, citrate, oxalate, lactate and phosphate are competitive binders for VO^{2+} in blood serum. The serum concentrations of these low molecular mass biogenic ligands amount to 0.01 mM for oxalate, 0.1 mM for citrate, 1.5 mM for lactate and 1.1 mM for phosphate.[29] The stability data for the ternary VO^{2+}-A^--B^{n-} systems (where A^- is 5MeOpic and B^{n-} the competitive ligand anion) are summarised in Table 7; for EPR data and ligand sets derived thereof see Table 4. Speciation diagrams are presented in Figure 5.

In the ternary system containing oxalate, the potentiometric titration curves could be fitted well by assuming the formation of two new complexes, $[VOAB]^-$ and

Table 7. Stability constants of mixed ligand VO^{2+} complexes at 25 °C and $I = 0.2$ M; VO^{2+}:HA:$H_nB = 1:2:2$; $c(V) = 1$ mM (3σ errors in parentheses).

Complex	Oxalate (B^{2-})	Lactate (B^-)	Citrate (B^{3-})	Phosphate (B^{3-})
$[VOABH_2]$	–	–	–	26.3(1)
[VOABH]	–	–	15.43(3)	22.70(7)
[VOAB]	11.33(1)	8.16(4)	11.84(3)	16.51(8)
$[VOABH_{-1}]$	3.89(5)	4.08(2)	7.38(2)	10.13(7)
fitting[a]	0.0092	0.0087	0.0102	0.0134
no. of points	296	314	316	248

[a] The average difference between the calculated and experimental titration curves expressed in mL of the titrant.

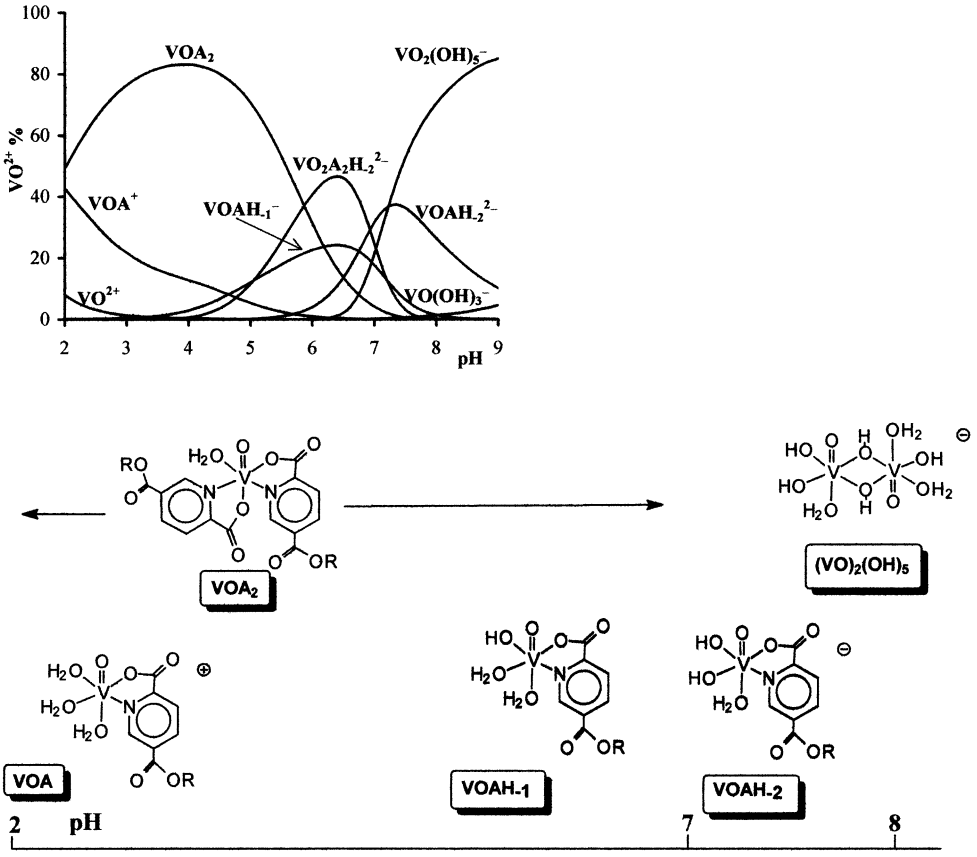

Figure 4. Speciation of the complexes formed in the VO^{2+}-AH system (AH = 5MeOpicH, **1a**) at a 1:4 metal-to-ligand ratio and $c(V) = 1$ mM.

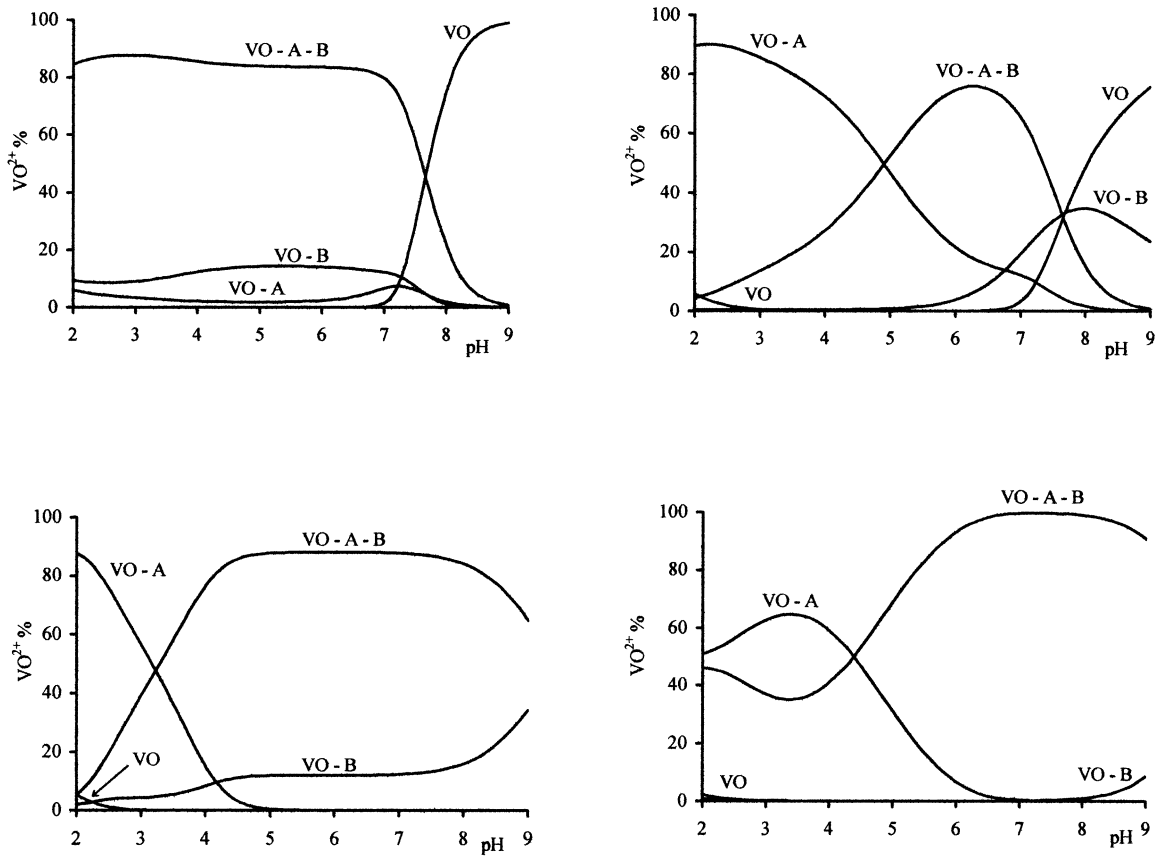

Figure 5. Speciation of the complexes formed in the VO^{2+}-AH-BH_n systems [$A^- = 5$ MeOpic, **1a**, B^{n-} (from top left to bottom right) = oxalate, lactate, citrate, phosphate] at a 1:2:2 (VO^{2+}:A^-:B^{n-}) ratio and $c(V) = 1$ mM.

$[VOH_{-1}AB]^{2-}$, dominating the pH range 2–8. The formation of the mixed complexes according to the reactions $VOA^+ + B^{2-} \rightarrow [VOAB]^-$ ($\log K = 6.17$) and $VOB + A^- \rightarrow [VOAB]^-$ ($\log K = 5.44$) is clearly favoured over the formation of the complexes $[VOB_2]^{2-}$ ($\log K = 4.79$[30]) and $[VOA_2]$ ($\log K = 4.36$). The EPR data indicate the presence of a single species (Table 4) over the pH range 2–7. The apparent contradiction with the speciation diagram (Figure 5), which indicates the simultaneous presence of about 15% of the species $[VOB_2]^{2-}$, can be explained with the very similar contributions of the CO_2^- and N_{aryl} donor atom sets to the parallel (z) component of the hyperfine coupling constant yielding basically the same A_z values for both the ternary species $[VOAB]^-$ and the binary bis(oxalato) complex $[VOB_2]^{2-}$. The recorded set of EPR parameters is in good agreement with those for the ternary complexes of pic ($g_z = 1.941$; $A_z = 167 \times 10^{-4}$ cm^{-1}) or 6Mepic ($g_z = 1.941$; $A_z = 166 \times 10^{-4}$ cm^{-1}), in both of which there is a *cis* arrangement of the ligand functions.[27, 28] This strongly suggests that $[VOAB]^-$ in the VO^{2+}-5MeOpicH system also features an equatorial {N_{aryl}, CO_2^-, CO_2^-, H_2O} donor set.

Lactate forms the ternary complexes [VOAB] and $[VOABH_{-1}]^-$, which are the major species in the pH range 4.5–7.5. The overall situation compares to that of the corresponding pic and 6Mepic systems, for which deprotonation of the alcoholic group of lactate was suggested for $[VOABH_{-1}]^-$.[31] Since the EPR parameters do not change significantly on deprotonation, the alcoholic group is supposedly in the axial position. The equatorial ligand set for both species is thus {N_{aryl}, CO_2^-, CO_2^-, H_2O}. The formation of ternary systems is also favoured with citrate. In this system, the curves can be fitted with the species $[VOABH]^-$, $[VOAB]^{2-}$ and $[VOABH_{-1}]^{3-}$. Based on the similarity of the EPR parameters in this system with those of the pic and 6Mepic systems,[27, 28] an equatorial ligand set {N_{aryl}, CO_2^-, CO_2^-, OH} is suggested for $[VOAB]^{2-}$ below pH ≈ 4, and {N_{aryl}, CO_2^-, CO_2^-, O^-} for $[VOABH_{-1}]^{3-}$ above pH ≈ 4, that is deprotonation and coordination of the alcoholic group. The significantly lower value of pK(VOAB) for 5MeOpic (4.42) compared to pic (5.76) or 6Mepic (5.66) indicates the more favoured formation of this complex in the VO^{2+}-5MeOpicH system. The decrease of A_z on going from $[VOAB]^{2-}$ (169) to $[VOABH_{-1}]^{3-}$ (159×10^{-4} cm^{-1}) confirms the presence of a stronger donor set for the latter. Ternary complexes [VOAHB] and $[VOAH_{-1}B]$ dominate with phosphate in the pH range 5–9. The practically constant EPR parameters suggest the same environment around the metal ion (only the protonation state of the phosphate is different) as was found for the corresponding complexes with pic.[28] Comparison of the pK($VOABH_{x)}$ (x = 2, 1) values for 5MeOpic (3.55 and 6.17) with those in the pic system (4.24 and 7.21) shows that the stepwise deprotonation of the mono-coordinated phosphate takes place at lower pH values for 5MeOpic, indicating somewhat stronger interaction between the metal ion and the ligand.

The speciation results indicate that, after absorption and transport into the blood, $[VO(5MeOpic)_2(H_2O)]$ (**2a**) under-

goes considerable transformations when it meets the more important low molecular mass bio-ligands of the blood serum. This is illustrated by the data in Table 8, which provides the distribution of VO^{2+} among picolinate and the four serum

Table 8. Species distribution of insulin-mimicking VO^{2+} picolinato complexes; calculated for $c(V) = 10\,\mu M$, phosphate 1.10 mM, citrate 99.0 μM, lactate 1.51 mM, and oxalate 9.20 μM; at pH 7.4.

VO^{2+} in	% VO^{2+} bound		
	[VO(5MeOpic)2]	[VO(6Mepic)2]	[VO(pic)2]
intact [VO(picolinate)$_2$]	0	0	0
ternary complexes with			
citrate	27	30	42
phosphate	14	0	0
binary complexes with			
citrate	50	61	50
lactate	9	9	8

ligands. The modelling calculations were performed at $c(VO^{2+}) = 10$ μM (this is a concentration level at which **2a** still shows a marked insulin-mimetic effect; see below), while the genuine serum concentrations were used for the bio-ligands. These findings indicate that both picolinato ligands are partly or completely displaced from the coordination sphere of VO^{2+}, mostly so by citrate, which binds 70–90% of the total VO^{2+} in binary or ternary complexes. Phosphate and lactate play a secondary role, and oxalate cannot compete. Preliminary calculations of the species distribution including the transport protein transferrin (Tf), using the VO^{2+}-Tf binding constants $\log K_1 = 13.2 \pm 0.8$[32] and $\log K_2 = 12.2 \pm 0.8$ (where K_1 was derived from the linear correlation between the first Tf binding constant and the first hydroxide binding constant of the metal ion,[33] and K_2 is based on the fact that the second Tf binding constant is usually smaller than the first one by one order of magnitude) show that about 65% of the vanadyl forms a binary complex with Tf, while the remaining approximately 35% are distributed between ternary vanadyl-5MeOpic-citrate and -phosphate species.

Insulin-mimetic and cytotoxicity tests: The biological tests for the determination of the insulin-mimetic abilities and the short term cell toxicity of **2a–d** were carried out on mice fibroblasts, transformed so as to exhibit a metabolism comparable to that of adipocytes.[4] $K[VO_2(pic)_2]$ and $K[VO_2(dipic)]$, the insulinmimetic behaviour of which has been established earlier (see Introduction), were included in these investigations.

For cytotoxicity tests, the fibroblasts were incubated with solutions of the vanadium complexes at different concentrations for 3 h. Trypan blue was then added, which stains living cells only. At concentrations of about 1 mM, the V^{IV} complexes caused morphological changes up to total lysis, while at concentrations of 0.1 mM and below, the compounds were non-toxic. The V^{V} picolinates were non-toxic even at 1 mM concentrations.

The insulin-mimetic tests on **2a–c**, $K[VO_2(pic)_2]$ and $K[VO_2(dipic)]$ with respect to uptake and degradation of glucose were performed by the MTT reduction essay. Soluble, yellow MTT is reduced in the last part of the mitochondrial electron transfer chain in living cells in to insoluble fomazan blue. Cells were incubated in an insulin-free medium for 24 h, followed by 3 h incubation with solutions of the vanadium compound. The amount of farmazan blue formed, determined photometrically, is proportional to the amount of glucose taken into and degraded within the cells. The results are represented in Figure 6. All of the compounds are effective at subtoxic concentrations; **1a**, $K[VO_2(pic)_2]$ and $K[VO_2(dipic)]$ are comparable to insulin itself.

The insulin-mimetic activity of ligand **1a** and complex **2a** was also studied with respect to the in vitro inhibition of the release of free fatty acids (FFA) from isolated rat adipocytes treated with epinephrine (adrenalin). Epinephrine activates lipases; the action of lipases in turn is counteracted by insulin. The results, presented in Figure 7, are compared with those of $VOSO_4$ ($[VO(OH)(H_2O)_4]^+$), VS, which is commonly used as a positive control and standard in these tests,[34] and $[VO(H_2O)(pic)_2]$. The inhibition was measured by the IC_{50} values, that is 50% inhibition concentration of a compound for the FFA release from adipocytes. Figure 7 shows the effect of **1a**, **2a**, VS and $[VO(pic)_2]$. Since **2a** exhibited a dose-dependent inhibitory effect as is the case with VS and $[VO(pic)_2]$, while the ligand **1a** alone showed no such effect, the apparent IC_{50} values (Table 9) were rated by comparison with VS ($IC_{50} =$ 1.0 mM). On the basis of IC_{50} values, complex **2a** has a substantially higher insulin-mimetic activity than VS. The difference in activities of **2a** and $[VO(pic)_2]$ was within the experimental error range, and also compares to that of the iodo derivative $[VO(5Ipic)_2(H_2O)]$.[11] The ligand **1a** itself is inactive.

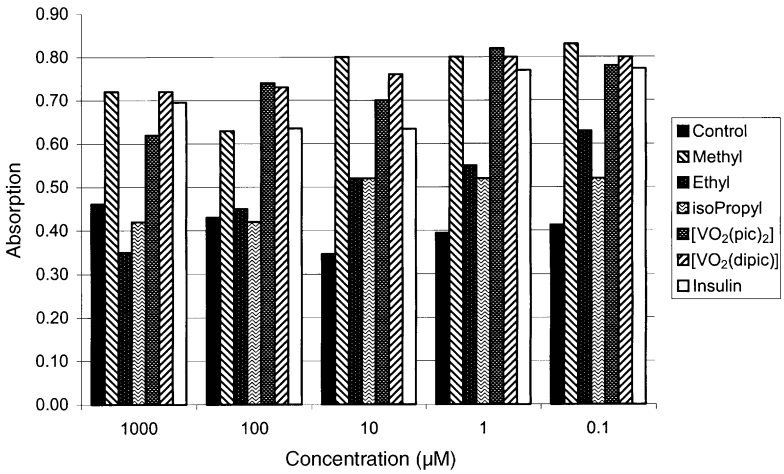

Figure 6. Glucose uptake stimulated by vanadium-picolinates. The absorbance is a measure of the efficacy of the compounds. The diagram also contains the data for a control group (neither insulin nor vanadium compound added), and for a group where insulin was employed instead of vanadium.

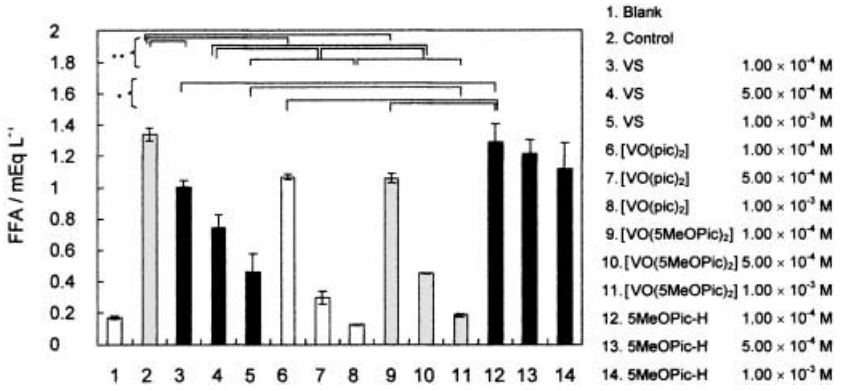

Figure 7. Inhibitory effect of vanadium complexes on fatty acid release from rat adipocytes treated with epinephrine (10^{-5} M; 3 h). Data are expressed as the mean ± SDs for three experiments. The blank corresponds to adipocytes without any treatment, the control to adipocytes pre-incubated with saline for 30 min. * and **: significance at $p < 0.05$ and 0.01, respectively.

Table 9. IC_{50} values

Compound	IC_{50} (mM)	SD
$VOSO_4$	1.00	0.16
1a	none	
2a	0.56	0.11
$[VO(pic)_2]$	0.48	0.08

Uptake of vanadium by fibroblasts: To assess the biological efficacy of a compound, its uptake by cells is an important feature. We have incubated SVT fibroblasts with 1M and 0.1M solutions of the compounds employed in the insulin-mimetic glucose uptake tests (**2a–c**, $K[VO_2(pic)_2]$, $K[VO_2(dipic)]$, including vanadate which is usually considered to penetrate cell walls easily through phosphate channels) and determined the cell vanadium contents by AAS after removal of the supernatant solutions and thorough washing of the cells. The results, collated in Table 10, have also been related to the cell mass as quantified by protein, determined by the BCA method (see Experimental Section). The data show that 3–15% of the vanadium in the original solution gets in the cells. The concentrations, in the micromolar range, are, however, still on a level relevant for physiological action. Interestingly,

Table 10. Vanadium uptake by SVT mice fibroblasts.[a]

Compound	μg Vanadium per L (concentration, μM)	ng V μg^{-1} protein[b]
2a, 1 mM	757 (14.8)	1.67
2a, 0.1 mM	73 (1.4)	0.12
2b, 0.1 mM	135 (2.6)	0.28
2b, 0.1 mM	21 (0.4)	0.03
2c, 0.1 mM	362 (7.1)	0.73
2c, 0.1 mM	37 (0.7)	0.06
$K[VO_2(pic)_2]$, 1 mM	431 (8.5)	0.79
$K[VO_2(pic)_2]$, 0.1 mM	42 (0.8)	0.07
$K[VO_2(dipic)]$, 1 mM	373 (7.3)	0.76
$K[VO_2(dipic)]$, 0.1 mM	68 (1.3)	0.14
$K[VO_3]$[c], 1 mM	373 (7.3)	0.76
$K[VO_3]$[c], 0.1 mM	68(1.3)	0.14

[a] Control < 10 μg V L^{-1}. [b] The average value of cell protein is 554 μg ml. [c] Present in solution as an equilibrium mixture mainly of $H_2VO_4^-$, $H_2V_2O_7^{2-}$ and $V_4O_{10}^{4-}$.

compound **2a**, which is clearly more effective than **2b** and **2c** in triggering intracellular glucose degradation (Figure 6), is also the one which is most effectively absorbed. The absorption is also better by a factor of two than for the anionic picolinato complexes and vanadate.

Conclusion

Two of the major functions of insulin are the activation of glucose uptake by glucose-metabolising cells from the blood serum, and the inhibition of lipolysis. Lacking insulin supply (diabetes 1) or insulin resistance (diabetes 2) leads to intolerable blood glucose levels and the formation of ketonic bodies which cause a variety of symptoms such as a malfunction of the peripheral blood circulation. Here we introduce a novel family of picolinatovanadium compounds for potential oral treatment of both types of diabetes mellitus. These compounds contain 5-carboalkoxypicolinates, which allow for a fine-tuning of the stability of the complexes and their lipophilicity/hydrophilicity. The complexes retain their identity under the acidic conditions encountered in the stomach. Under pH conditions pertinent to the blood (7.35), mainly vanadyl hydroxides form. However, in the presence of the biogenic blood constituents citrate and phosphate (and, to a certain extent, also oxalate and lactate), stable ternary complexes form that still contain the specifically designed picolinate derivative and should be considered the active forms of the vanadium complexes in insulin mimesis. In particular, the complex of the methyl ester, $[VO(H_2O)(5\text{-MeOpic})_2]$ (**2a**)—or essentially [VO(5MeOpic)citrate]$^{n-}$ under physiological conditions—effectively mimics insulin in vitro with respect to glucose uptake by mice fibroblasts and inhibition of lipolysis (release of free fatty acids) by rat adipocytes. **2a** is more effectively taken up by fibroblasts than the more lipophilic ethyl and isopropyl ester compounds (**2b** and **2c**), and the more hydrophilic anionic picolinato complexes. **2a** is thus expected to exhibit in vivo normoglycemic activity.

Experimental Section

Instrumentation: Infrared spectra were recorded as KBr pellets on a Perkin Elmer 1720 FTIR spectrometer and NMR spectra were recorded on a Varian Gemini 200 BB spectrometer at room temperature, relative to TMS for ^{1}H (200 MHz) and ^{13}C (50 MHz), and relative to external $VOCl_3$ for ^{51}V (53 MHz). EPR spectra were run in the X-band mode (9.75 MHz) on a BrukerESP 300E spectrometer. Simulations were carried out with the program system SimFonia. Mass spectrometry was carried out with the usual spectrometer settings (70 eV, EI/FAB) on a Varian MAT 311A (70 eV, EI) or a VG Analytical 70-250S (FAB) instrument. The thermogravimetric analysis of **2a** was carried out with an STA 409 instrument (Netzsch), coupled to a quadrupole mass spectrometer QMG 421 (Balzers)

with a heating program of 5 K min^{-1} between 30 and 850 °C. pH-Potentiometric measurements were performed with a radiometer pHM 84 equipped with a Metrohm combined electrode (type 6.0234.110), calibrated for hydrogen ion concentration according to Irving.[36]

X-ray structure analyses were carried out at 153(2) K using $Mo_{K\alpha}$ radiation ($\lambda = 0.71073$ Å, graphite monochromator) on a Smart Apex CCD diffractometer at 153(2) K. Hydrogen atoms were usually found and refined anisotropically, and otherwise calculated into idealised positions and included in the last cycles of refinement. Absorption corrections were carried out by SADABS. Disorder information: **2a**·3.5 H_2O: In one of the two independent molecules, the carbomethoxy group (C32O19) disordered over two positions was treated with a 0.7:0.3 model. Four of the seven water molecules of crystallisation showed partial occupancy/were disordered and were dealt with by employing the following REM: O24 0.5, O25/O26 0.75/0.25, O27/O28 0.65/0.35, O29/O30 0.3/0.2, O31/O32/O33/O35 0.35/0.30/0.20/0.15. **3**: Disorder of 1 H_2O per 0.5 V; REM = O11 0.18, O12 0.12, O13 0.06, O14 0.15, O15 0.05, O16 0.10, O17 0.15, O18 0.07, O19 0.05, O20 0.07. For crystal data and structure refinement see Table 11.
CCDC-207528(**1b**), CCDC-207529 (**1a**·H_2O), CCDC-207530 (**1c**), CCDC-207531 ([NH_4]**3**·4 H_2O), CCDC-207532 (**2a**·3.5 H_2O) contain the supplementary crystallographic data for this paper. These data can be obtained free of charge via www.ccdc.cam.ac.uk/conts/retrieving.html (or from the Cambridge Crystallographic Data Centre, 12, Union Road, Cambridge CB2 1EZ, UK; fax: (+44) 1223-336-033; or deposit@ccdc.cam.ac.uk).

Potentiometric measurements: The stability constants of the proton and VO^{2+} complexes of the ligands were determined by pH-potentiometric titration of 20.0 mL samples. The picolinic acid (5MeOpicH, A) concentration was in the range 2–6 mM, and the molar ratios in the VO^{2+}-A system were 0:1, 1:1, 1:2, 1:4. For the ternary systems containing lactate, oxalate, phosphate or citrate, B, the VO^{2+}:A:B ratios were 1:1:1, 1:1:2, 1:2:1, or 1:2:2. All of the titrations were performed over the pH range 2–11, or until precipitation occurred, with a carbonate-free KOH solution of known concentration (≈0.2 M), under a purified argon atmosphere. The reproducibility of the titration points included in the evaluation was within 0.005 pH units over the whole pH range. A pK_w value of 13.76 ± 0.01 was determined and used for the calculations. The concentration stability constants $\beta_{pqr} = [M_pH_qA_r]/[M]^p[H]^q[A]^r$ for binary complexes and $\beta_{pqrs} = [M_pH_qA_rB_s]/[M]^p[H]^q[A]^r[B]^s$ for ternary species were calculated with the PSEQUAD computer program.[37] The uncertainties (3σ values) of the stability constants are given in parentheses in the tables. During the calculations the following VO^{2+}-hydroxo complexes were assumed: $[VO(OH)]^+$ ($\log_{1,-1,0} = -5.94$), $[\{VO(OH)\}_2]^{2+}$ ($\log_{2,-2,0} = -6.95$), calculated from the data published by Henry et al.,[38] the Davie's equation being used to take into consideration the different ionic strengths, $[VO(OH)_3]^-$ ($\log_{1,-3,0} = -18.0$) and $[(VO)_2(OH)_5]^-$ ($\log_{2,-5,0} = 22.5$) taken from ref. [39]. The ionic strength was adjusted to 0.20 M KCl in each solution studied. In all cases, the temperature was maintained at 25.0 ± 0.1 °C.

Toxicity and insulin-mimetic tests: Cytotoxicity and glucose uptake tests were performed on Simian virus modified Swiss 3T3 mice fibroblasts (cell line SV 3T3), maintained as described elsewhere.[4] SV modified fibroblasts attain metabolic properties closely related to adipocytes and are thus particularly suited in studies of glucose uptake and metabolism. For the tests, cells were grown to sub-confluency. For toxicity tests, the cells, kept in Dulbecco's modification of Eagle's medium (DMEM, Sigma), were incubated with solutions of the vanadium compounds for 3 h. The supernatant medium was removed. Trypan blue (0.2% w/v) in phosphate-buffered saline solution was added, and the ratio of stained and non-stained cells determined after 5 min. Tests for the glucose uptake activity were based on the MTT reduction essay. We have shown previously that the results obtained by the MTT test are compatible with direct measurements of the uptake of tritium labelled glucose.[4] The cells were incubated in insulin-free, supplemented[4] DMEM medium for 24 h. DMEM (without phenol red) supplemented with MTT (Sigma; 0.5 g L^{-1}) and the solution of the vanadium complex were added to the cells and incubated for 3 h at 37 °C in a 5% CO_2 atmosphere. The reaction was then stopped by addition of 0.05 M HCl in 2-propanol. The dye was extracted with HCl/2-propanol, and the amount of formazan blue formed by reduction of MTT was measured at 570 nm in a multi-well reader (SLT 340 ATC).

For determination of the vanadium uptake by the fibroblasts, the cells were pre-treated accordingly (3 h of incubation with the solutions of the vanadium complexes) on micro-well plates. The supernatant was discarded, the cells washed twice with buffer, treated with 1 mL of 0.5 M NaOH per well and stirred over night to ascertain complete digestion. Half of each sample was then subjected to AAS (graphite tube) on a PE 4100ZL instrument. For the analyses, 20 μL sample volumes were employed, acidified with HNO_3 and 5 μg Pd + 3 μg $MgNO_3$ added as modifier.

Table 11. Crystal data and structure refinement for **1a**·H_2O, **1b**, **1c**, **2a**·3.5 H_2O and [NH_4]-**3**·4 H_2O.

	1a·H_2O	**1b**	**1c**	**2a**·3.5 H_2O	[NH_4]-**3**·4 H_2O
empirical formula	$C_8H_9NO_5$	$C_9H_9NO_4$	$C_{10}H_{11}NO_4$		$C_{16}H_{24}N_3O_{14}V$
M [g mol^{-1}]	199.16	195.17	209.20		533.32
crystal system	triclinic	triclinic	monoclinic	triclinic	monoclinic
space group	$P\bar{1}$	$P\bar{1}$	$P2(1)/c$	$P\bar{1}$	$C2/c$
cell dimensions					
a [Å]	7.1533(12)	9.4412(3)	12.3015(4)	13.0348(8)	18.121(3)
b [Å]	7.2375(12)	10.8428(4)	9.2940(3)	13.3654(8)	15.169(2)
c [Å]	9.5728(16)	13.4610(5)	8.9091(3)	15.1968(10)	10.0449(15)
α [°]	81.499(3)	102.5600(10)	90	104.607(1)	
β [°]	76.958(2)	97.8760(10)	95.4080(10)	100.850(1)	119.233(2)
γ [°]	65.886(2)	97.5560(10)	90	116.090(1)	
V [[Å]^3/Z]	439.82(13)/2	1313.65(8)/6	1014.04(6)/4	2156.4(2)/4	2409.5(6)/4
ρ_{calcd} [g cm^{-3}]	1.504	1.480	1.370	1.568	1.470
μ [mm^{-1}]	0.127	0.118	0.107	0.534	0.484
F(000)	208	612	440	1043	1104
crystal size [mm]	0.75 × 0.20 × 0.05	0.80 × 0.70 × 0.30	0.65 × 0.53 × 0.34	0.05 × 0.05 × 0.15	0.43 × 0.31 × 0.17
θ range [°]	2.19–27.53	2.19–32.00	2.75–31.99	1.48–25.02	2.44–27.49
index ranges	$-9 < h < 9$ $-14 < h < 14$	$-13 < h < 18$	$-15 < h < 15$	$-23 < h < 23$	
	$-9 < k < 9$	$-16 < k < 16$	$-11 < k < 13$	$-15 < k < 15$	$-19 < k < 19$
$-12 < l < 12$	$-20 < l < 20$	$-13 < l < 13$		$-18 < l < 18$	$-13 < l < 13$
reflections collected	5058	34668	14255	21985	14245
independent reflections (R_{int})	1973 (0.0268)	8881 (0.0550)	3457 (0.0274)	7577 (0.0881)	2750 (0.0302)
restraints/parameters	0/140	0/388	0/140	1/599	4/190
GooF on F^2	1.019	1.020	1.089	0.840	1.038
final R ($I > 2\sigma I_0$), $R1$/$wR2$	0.0417/0.1116	0.0600/0.1524	0.0491/0.1445	0.0561/0.1325	0.0445/0.1275
R indices (all data), $R1$/$wR2$	0.0488/0.1154	0.0770/0.1619	0.0555/0.1481	0.1348/0.1814	0.0533/0.1317
largest diff. peak and hole [e Å^{-3}]	0.236/−0.0229	0.680/−0.429	0.490/−0.202	0.624/−0.482	0.516/−0.264

Calibration was carried out against a 0.5 M NaOH solution containing 100 μg V and 500 mg BSA (bovine serum albumin) per L. The second half of each sample of the digested cell material was subjected to protein determination by the BCA (bicinechoninic acid) method on 10 μL samples. Calibration was carried out against 10 μL samples of a BSA dilution sequence.

Tests for the inhibition of free fatty acid (FFA) release were performed on rat adipocytes. Male Wistar rats were killed by bleeding under anaesthesia with ether (animal experiments were approved by the Experimental Animal Research Committee of Kyoto Pharmaceutical University and performed according to the guidelines), and adipose tissues were removed, chopped, and digested with collagenase for 1 h at 37 °C in Krebs-Ringer bicarbonate buffer, pH 7.4, containing 2% bovine serum albumin. The adipocytes thus obtained were separated from undigested tissue by filtration through nylon mesh, and washed three times with collagenase free buffer. 15 μL of saline glucose solution and 30 μL of the vanadium complexes dissolved in saline/DMSO were added to 240 μL (10^6 cells mL^{-1}) of isolated adipocytes, and the resulting suspensions pre-incubated at 37 °C for 30 min. After addition of 15 μL of 0.2 mM epinephrine dissolved in saline, the resulting mixture was incubated (37 °C, 3 h). The reaction was stopped by cooling with ice-water. The FFA concentration in the outer solution of the cells was determined by an NEFA kit (Wako Pure Chemicals). Final concentrations were as follows: glucose 5 mM; vanadium compounds 0.1, 0.5 and 1 mM; ligand **1a** 0.2, 1 and 2 mM; epinephrine 0.01 mM; DMSO 2% v/v.

Reagents and general: Vanadylsulfate $VOSO_4 \cdot 5H_2O$, $[NH_4][VO_3]$ and pyridin-2,5-dicarboxylic acid were obtained from Merck and Fluka and used without further purification. $K[VO_2(dipic)]$ was prepared as described,[40], and $K[VO_2(pic)_2]$ was obtained in analogy to the respective ammonium salt.[18] Oxalate, lactate, citrate and phosphate were Aldrich products of puriss. quality (≥ 98.5%) and used as received. Their purities were checked and the exact concentrations of the prepared stock solutions were determined by the Gran method.[41] VO^{2+} stock solution was prepared according to Nagypál and Fábián[42] and standardised for metal ion concentration by permanganate titration and for hydrogen ion concentration by pH-potentiometry, using the appropriate Gran function.

All syntheses with vanadium in oxidation state +IV were carried out under an atmosphere of nitrogen using Schlenk techniques. Tetrahydrofuran (THF) was dried and deoxygenated by refluxing for 3 h over $LiALH_4$, and distilled in an N_2 stream. Deionised water was degassed before use.

Syntheses of compounds

General procedure for the 5-carboalkoxypicolinates 1a–d (see also Scheme 1): The syntheses of the dialkylesters from dipicolinic acid via the acid dichloride followed literature procedures.[13] Synthesis of the monoesters was carried out according to Ooi and Magee,[14] with the modification that a molar ratio diester to copper(II)nitrate of 1:1 was chosen and the reaction mixture kept at reflux for 3 h to yield the blue copper complexes $[Cu(5ROpic)_2]$, from which the ligands were liberated with H_2S. The ligands were isolated as white or slightly yellow solids in yields of 44 to 72%.

5-Carbomethoxypyridine-2-carboxylic acid, 5MeOpicH (1a): IR (KBr): $\tilde{\nu} = 3089$, 3011 (ar. C–H); 2967 (CH_3); 1719 (C=O); 1698 (C=O); 1594, 1570, 1484 (C=C), (C=N); 1421, 1383 (CH_3), (OH); 1309, 1289, 1255 (C=C), (C=N); 1115, 1020 (O–CH_3); 746 cm^{-1} (ar. C–H); ^1H NMR ([D$_6$]DMSO, TMS): $\delta = 9.22$ (dd, $^4J_{6,4} = 1.89$ Hz, $^5J_{6,3} = 0.85$ Hz, 1H; H-6), 8.56 (dd, $^4J_{4,6} = 1.89$ Hz, $^3J_{4,3} = 8.13$ Hz, 1H; H-4), 8.32 (dd, $^5J_{3,6} = 0.85$ Hz, $^3J_{3,4} = 8.13$ Hz, 1H; H-3), 4.02 ppm (s, 3H; CH_3); ^{13}C NMR ([D$_6$]DMSO, TMS): $\delta = 165.40$ (C-2′), 164.52 (C-5′), 151.62 (C-2), 149.70 (C-6), 138.24 (C-4), 127.82 (C-5), 124.54 (C-3), 52.68 ppm (OCH_3); elemental analysis calcd (%) for $C_8H_7NO_4 \cdot H_2O$ (199.16): C 48.25, H 4.55, N 7.03; found: C 48.21, H 4.35, N 7.02; MS (70 eV, EI): *m*/*z* (%): 181 (2) [$M^{+\bullet}$], 150 (49) [$M - CH_3O$], 137 (100) [$M - CO_2$], 122 (30) [$M - C_2H_3O_2$], 106 (16) [$M - C_2H_3O_3$], 78 (17) [C_5H_4N].

5-Carboethoxypyridine-2-carboxylic acid, 5EtOpicH (1b): IR (KBr): $\tilde{\nu} =$ 3131 (ar. C–H); 2984, 2943, 2821 (CH); 1718 (C=O); 1601, 1577 (C=C), (C=N); 1476, 1440, 1383, 1371 (CH), (OH); 1302, 1279, 1247 (C=C), (C=N); 1118, 1028 (C–O); 748 cm^{-1} (ar. C–H); ^1H NMR ([D$_6$]DMSO): $\delta = 9.15$ (d, $^5J_{6,3} = 1.28$ Hz, 1H; H-6), 8.44 (dd, $^4J_{4,6} = 2.01$ Hz, $^3J_{4,3} = 8.06$ Hz, 1H; H-4), 8.15 (d, $^3J_{3,4} = 8.06$ Hz, 1H; H-3), 4.37 (q, $^3J = 7.11$ Hz, 2H; CH_2CH$_3$), 1.34 ppm (t, $^3J = 7.11$ Hz, 3H; CH$_2$CH_3); ^{13}C NMR ([D$_6$]DMSO): $\delta = 165.48$ (C-2′), 164.07 (C-5′), 151.66 (C-2), 149.75 (C-6), 138.24 (C-4), 128.10 (C-5), 124.62 (C-3), 61.65 (CH_2CH$_3$), 14.16 ppm (CH$_2$CH_3); elemental analysis calcd (%) for $C_9H_9NO_4$ (195.17): C 55.39, H 7.18, N 4.65; found: C 55.27, H 7.16, N 4.55; MS (70 eV, EI): *m*/*z* (%): 195 (2) [$M^{+\bullet}$], 151 (100) [$M - CO_2$], 150 (79) [$M - C_2H_5O$], 123 (37) [$M - C_3H_4O_2$], 106 (12) [$M - C_3H_5O_3$], 78 (14) [C_5H_4N].

5-Carboisopropoxypyridine-2-carboxylic acid, 5iPrOpicH (1c): IR (KBr): $\tilde{\nu} =$ 3053 (ar. C – H); 2980, 2875, 2767 (CH); 1718 (C=O); 1600, 1583, 1498 (C=C), (C=N); 1459, 1471, 1377 (CH), (OH); 1301, 1269 (C=C), (C=N); 1108, 1036 (C–O); 750 cm^{-1} (ar. C–H); ^1H NMR ([D$_6$]DMSO): $\delta = 9.12$ (dd, $^4J_{6,4} = 2.17$ Hz, $^5J_{6,3} = 0.82$ Hz, 1H; H-6), 8.40 (dd, $^4J_{4,6} = 2.17$ Hz, $^3J_{4,3} =$ 8.10 Hz, 1H; H-4), 8.13 (dd, $^5J_{3,6} = 0.82$ Hz, $^3J_{3,4} = 8.10$ Hz, 1H; H-3), 5.16 (e, $^3J = 6.23$ Hz, 1H; CH(CH$_3$)$_2$), 1.32 ppm (d, $^3J = 6.23$, 6H; CH(CH_3)$_2$); ^{13}C NMR ([D$_6$]DMSO): $\delta = 166.17$ (C-2′), 164.21 (C-5′), 152.32 (C-2), 150.39 (C-6), 138.82 (C-4), 128.98 (C-5), 125.24 (C-3), 69.95 (CH(CH$_3$)$_2$), 22.21 ppm (CH(CH_3)$_2$); elemental analysis calcd (%) for $C_{10}H_{11}NO_4$ (209.20): C 57.41, H 5.30, N 6.70; found: C 57.34, H 5.31, N 6.67; MS (70 eV, EI): *m*/*z* (%): 209 (5) [$M^{+\bullet}$], 168 (42) [$M - C_3H_5$] , 165 (34) [$M -$ CO_2], 150 (100) [$M - C_3H_7O$], 123 (41) [$M - C_4H_6O_2$], 43 (21).

5-Carbo(*R*,*S*)-secbutylmethoxypyridine-2-carboxylic acid, 5sBuOpicH (1d): IR (KBr): $\tilde{\nu} = 3047$ (ar. C–H); 2976, 2935, 2878, 2768 (CH); 1715 (C=O); 1599, 1581 (C=C), (C=N); 1457, 1419, 1372 (CH), (OH); 1297, 1267 (C=C), (C=N); 1119, 1109, 1035 (C–O); 749 cm^{-1} (ar. C–H); ^1H NMR ([D$_6$]DMSO, TMS): $\delta = 9.17$ (br, 1H; H-6), 8.46 (d, $^3J_{4,3} = 8.06$ Hz, 1H; H-4), 8.19 (br, 1H; H-3), 5.06 (ps, $J = 6.23$ Hz, 1H; CH(CH$_3$)CH$_2$CH$_3$), 1.78–1.64 (m, 2H; CH(CH$_3$)CH_2CH$_3$), 1.33 (d, $J = 6.23$ Hz, 3H; CH(CH_3)CH$_2$CH$_3$), 0.94 ppm (t, $^3J = 7.42$ Hz, 3H; CH(CH$_3$)CH$_2$CH_3); ^{13}C NMR ([D$_6$]DMSO/TMS): $\delta = 165.87$ (C-2′), 163.84 (C-5′), 151.9 (C-2), 148.88 (C-6), 138.26 (C-4), 128.26 (C-5), 124.75 (C-3), 73.63 (CH(CH$_3$)CH$_2$CH$_3$), 28.26 (CH(CH$_3$)CH_2CH$_3$), 19.21 (CH(CH_3)CH$_2$CH$_3$), 9.53 ppm (CH(CH$_3$)CH$_2$CH_3); elemental analysis calcd (%) for $C_{11}H_{13}NO_4$ (223.23): C 59.19, H 5.87, N 6.27; found: C 58.88, H 5.91, N 6.31; MS (70 eV, EI): *m*/*z* (%): 223 (1) [$M^{+\bullet}$], 168 (60) [$M - C_4H_7$], 150 (100) [$M - C_4H_9O$], 122 (25) [$M - C_5H_9O_2$].

General procedure for the preparation of the vanadium compounds [VO(H$_2$O)(5ROpic)$_2$] (2a–d): A solution of $VOSO_4 \cdot 5H_2O$ (127 mg, 0.5 mmol) in H_2O (2 mL) was added to a solution of 5ROpicH (1.0 mmol) and $NaO_2CCH_3 \cdot 3H_2O$ (136 mg, 1.0 mmol) in water (10 mL) plus THF (1 mL). After 2 h of stirring at 50 °C, a green precipitate was formed which was isolated by filtration and dried in vacuo. Yields ranged from 60 to 85%.

[VO(H$_2$O)(5MeOpic)$_2$] (2a): IR (KBr): $\tilde{\nu} = 3115$, 3070 (ar. C–H); 2958 (CH_3); 1733 (C=O); 1654 (CO_2^-); 1578 (C=C), (C=N); 1439, 1397 (CH_3), (CO_2^-); 1303, 1286 (C=C), (C=N); 1124, 1045 (O–CH_3); 971 (V=O); 833 (ar. C–H), (C–CO_2); 750 cm^{-1} (ar. C–H); elemental analysis calcd (%) for $C_{16}H_{14}N_2O_{10}V$ (445.23): C 43.16, H 3.17, N 6.29 V 11.68; found: C 42.50, H 3.30, N 6.27, V 11.44; MS (FAB): *m*/*z* (%): 428.

[VO(H$_2$O)(5EtOpic)$_2$] (2b): IR (KBr): $\tilde{\nu} = 3120$, 3059 (ar. C–H); 2980, 2936, 2919 (C–H); 1737 (C=O); 1651 (CO_2^-); 1610, 1574 (C=C), (C=N); 1489, 1402, 1364 (CH), (CO_2^-); 1294 (C=C), (C=N); 1121, 1045 (C–O); 978 (V=O); 849 (ar. C–H), (C–CO_2); 753 cm^{-1} (ar. C–H); elemental analysis calcd (%) for $C_{18}H_{18}N_2O_{10}V \cdot 0.5H_2O$ (482.29): C 44.83, H 3.97, N 5.81; found: C 45.03, H 3.98, N 5.53; MS (FAB): *m*/*z* (%): 456.

[VO(H$_2$O)(5iPrOpic)$_2$] (2c): IR (KBr): $\tilde{\nu} = 3114$, 3058 (ar. C–H); 2983, 2873 (C–H); 1730 (C=O); 1687, 1652 (CO_2^-); 1609 (C=C), (C=N); 1484, 1397, 1353 (CH), (CO_2^-); 1289 (C=C), (C=N); 1108, 1051 (C–O); 967 (V=O); 848 (ar. C–H), (C–CO_2); 750 cm^{-1} (ar. C–H); elemental analysis calcd (%) for $C_{20}H_{22}N_2O_{10}V$ (501.34): C 47.91, H 4.42, N 5.59; found: C 47.56, H 4.45, N 5.08; MS (FAB): *m*/*z* (%): 484.

[VO(H$_2$O)(5sBuOpic)$_2$] (2d): IR (KBr): $\tilde{\nu} = 3118$, 3058 (ar. C–H); 2975, 2927 (C–H); 1729 (C=O); 1650 (CO_2^-); 1576 (C=C), (C=N); 1485, 1458, 1403, 1358 (CH), (CO_2^-); 1293 (C=C), (C=N); 1125, 1049 (C–O); 967 (V=O); 851 (ar. C–H), (C–CO_2); 750 cm^{-1} (ar. C–H); elemental analysis calcd (%) for $C_{22}H_{26}N_2O_{10}V$ (529.40): C 49.91, H 4.95, N 5.29; found: C 49.64, H 5.10, N 5.29; MS (FAB): *m*/*z* (%): 512.

[NH$_4$][VO$_2$(5MeOpic)$_2$] (3): A solution of 5MeOpicH (182 mg, 1.0 mmol) in acetone (1 mL) was added to a slurry of $[NH_4][VO_3]$ (59 mg, 0.5 mmol) in water (0.5 mL). The resulting yellow solution was stirred overnight and kept at 4 °C for two days. Yellow single crystals of [NH$_4$]-**3**$\cdot 4H_2O$ were obtained from the reaction solution by further cooling. Elemental analyses were not carried out due to very low yields of pure, crystalline material. IR

(KBr): $\tilde{\nu}$ = 3114, 3081 (ar. C–H); 2963 (CH_3); 1732 (C=O); 1658 (CO_2^-); 1580 (C=C), (C=N); 1439, 1396 (CH_3), (CO_2^-); 1348, 1304, 1283 (C=C), (C=N); 1125, 1037 (O–CH_3); 903 (V=O); 836 (ar. C–H), (C–CO_2); 751 cm^{-1} (ar. C–H); ^{1}H NMR (D_2O): δ = 9.05–7.95 (m, 3H; H-6, H-4, H-3), 3.95 ppm (s, 3H; CH_3); ^{51}V NMR (D_2O): δ = –575 ppm.

Acknowledgement

This work was supported by the Deutsche Forschungsgemeinschaft, the Fonds der Chemischen Industrie, the European COST Programme D21-0009-01 and the Hungarian Scientific Fund (OTKA T31896, F32235). P.B. gratefully acknowledgements the János Bólyai research fellowship for financial support. We also thank Marion Eternot (SOKRATES student from the Universitée Pierre et Marie Curie, Paris) and A.-Lüder Gaulke, University of Hamburg, for support with the syntheses.

[1] B. Lyonnet, X. Mertz, E. Martin, *Presse Med.* **1899**, *1*, 191.
[2] K. H. Thompson, J. H. McNeill, C. Orvig, *Chem. Rev.* **1999**, *99*, 2561–2571.
[3] H. Sakurai, Y. Kojima, Y. Yoshikawa, K. Kawabe, H. Yasui, *Coord. Chem. Rev.* **2002**, *226*, 187–198.
[4] D. Rehder, J. Costa Pessoa, C. F. G. C. Geraldes, M. M. C. A. Castro, T. Kabanos, T. Kiss, B. Meier, G. Micera, L. Pettersson, M. Ranger, A. Salifoglou, I. Turel, D. Wang, *J. Biol. Inorg. Chem.* **2002**, *7*, 384—396.
[5] D. C. Crans, *J. Inorg. Biochem.* **2000**, *80*, 123–131 and references therein.
[6] M. Melchior, S. J. Rettig, B. D. Liboiron, K. H. Thompson, V. G. Yuen, J. H. McNeill, C. Orvig, *Inorg. Chem.* **2001**, *40*, 4686–4690.
[7] P. J. Stankiewicz, A. S. Tracey, D. C. Crans, *Vanadium and Its Role in Life* (Eds.: H. Sigel, A. Sigel), Metal Ions in Biological Systems, *vol. 31,* Marcel Dekker, New York **1995**, ch. 9.
[8] J. Selbin, *Coord. Chem. Rev.* **1966**, *1*, 293–314.
[9] H. Sakurai, K. Fujii, H. Watanabe, H. Tamura, *Biochem. Biophys. Res. Commun.* **1995**, *214*, 1095–1101.
[10] S. Fujimoto, K. Fujii, H. Yasui, R. Matsushita, J. Takada, H. Sakurai, *J. Clin. Biochem. Nutr.* **1997**, *23*, 113–129.
[11] T. Takino, H. Yasui, A. Yoshitake, Y. Hamajima, R. Matsushita, J. Takada, H. Sakurai, *J. Biol. Inorg. Chem.* **2001**, *6*, 133–142.
[12] G. R. Willsky, A. B. Goldfine, P. J. Kostyniak, J. H. McNeill, L. Yaang, H. R. Khan, D. C. Crans, *J. Inorg. Biochem*. **2001**, *85*, 33–42.
[13] J. V. Fondacaro, D. S. Greco, D. C. Crans, *Annu. Vet. Med. Forum* **1999**, 710.
[14] T. Sasagawa, Y. Yoshikawa, K. Kawabe, H. Sakurai, Y. Kojima, *J. Inorg. Biochem.* **2002**, *88*, 108–112.
[15] H. Yasui, A. Tamura, T. Takino, H. Sakurai, *J. Inorg. Biochem.* **2002**, *91*, 327–338.
[16] L. Yang, A. La Cour, O. P. Anderson, D. C. Crans, *Inorg. Chem*. **2002**, *41*, 6322–6331.
[17] D. C. Crans, L. Yang, J. A. Alfano, L.-H. Chi, W. Jin, M. Mahroof-Tahir, K. Robbins, M. M. Toloue, L. K. Chan, A. J. Plante, R. Z. Grayson, G. R. Willsky, *Coord. Chem. Rev.* **2003**, *237*, 13–22.
[18] M. Melchior, K. H. Thompson, J. M. Jong, S. J. Rettig, E. Shuter, V. G. Yuen, Y. Zhou, J. H. McNeill, C. Orvig, *Inorg. Chem.* **1999**, *38*, 2288–2293.
[19] D. C. Crans, L. Yang, T. Jakusch, T. Kiss, *Inorg. Chem.* **2000**, *39*, 4109–4416.
[20] D. S. Greco, *Diabetes* **1997**, *46*, 1289.
[21] A. Shaver, J. B. Ng, D. A. Hall, B. S. Lum, B. I. Posner, *Inorg. Chem.* **1993**, *32*, 3109–3113.
[22] L. Yang, D. C. Crans, S. M. Miller, A. La Cour, O. P. Anderson, P. M. Kaszynski, L. D. Austin, G. R. Willsky, *J. Am. Chem. Soc.* **2002**, *41*, 4859–4871.
[23] T. H. Fife, T. J. Przystas, *J. Am. Chem. Soc.* **1982**, *104*, 2225–2257.
[24] G. K. S. Ooi, R. J. Magee, *J. Inorg. Nucl. Chem.* **1970**, *32*, 3315–3320.
[25] a) M. R. Maurya, S. Khurana, Shailendra A. Azam, W. Zhang, D. Rehder, *Eur. J. Inorg. Chem.* **2003**, 1966–1973; b) M. R. Maurya, S. Khurana, W. Zhang, D. Rehder, *J. Chem. Soc. Dalton Trans.* **2002**, 3015–3023.
[26] N. D. Chasteen, *Biological Magnetic Resonance, vol. 3* (Eds.: L. J. Berliner, J. Reuben), Plenum, New York, **1981**.
[27] T. Kiss, E. Kiss, E. Garriba, H. Sakurai, *J. Inorg. Biochem.* **2000**, *80*, 65–73.
[28] E. Kiss, E. Garribba, G. Micera, T. Kiss, H. Sakurai, *J. Inorg. Biochem*. **2000**, *78*, 97–108.
[29] W. R. Harris, *J. Clin. Chem.* **1992**, *38*, 1809–1818.
[30] P. Buglyó, E. Kiss, I. Fábián, T. Kiss, D. Sanna, E. Garribba, G. Micera, *Inorg. Chim. Acta* **2000**, *306*, 174–183.
[31] T. Kiss, P. Buglyó, D. Sanna, G. Micera, P. Decock, D. Dewaele, *Inorg. Chim. Acta* **1995**, *239*, 145–153.
[32] T. Kiss, *Abstracts of the 6th European Conference of Bioinorganic Chemistry*, Lund and Copenhagen, **2002**, p. 48.
[33] H. Sun, M. C. Cox, H. Li, P. Sadler, *Struct. Bonding (Berlin)*, **1997**, *88*, 71.
[34] M. Nakai, H. Watanabe, C. Fujiwara, H. Kakegawa, T. Satoh, T. Takada, R. Matsushita, H. Sakurai, *Biol. Pharm. Bull.* **1995**, *18*, 719–725.
[35] K. Elvingson, A. Gonzáles-Baró, L. Pettersson, *Inorg. Chem*. **1996**, *35*, 3388–3393.
[36] H. M. Irving, M. G. Miles, L. D. Pettit, *Anal. Chim. Acta,* **1967**, *38*, 475–488.
[37] L. Zékány, I. Nagypál in *Computational Methods for the Determination of Stability Constants* (Ed.: D. Leggett), Plenum, New York, **1985**.
[38] R. P. Henry, P. C. H. Mitchell, J. E. Prue, *J. Chem. Soc. Dalton Trans.* **1973**, 1156–1159.
[39] A. Komura, M. Hayashi, H. Imanaga, *Bull. Chem. Soc. Jpn*. **1977**, 2927–2931.
[40] K. Wieghardt, *Inorg. Chem.* **1978**, *17*, 57–64.
[41] G. Gran, *Acta Chem. Scand.* **1950**, *4*, 559–577.
[42] I. Nagypál, I. Fábián, *Inorg. Chim. Acta* **1982**, *61*, 109–113.

Received: April 7, 2003 [F5019]

